Temperature-dependence of mitochondrial function and production of reactive oxygen species in the intertidal mud clam *Mya arenaria*

D. Abele[1,*], K. Heise[1], H. O. Pörtner[1] and S. Puntarulo[2]

[1]*Alfred Wegener Institut for Polar and Marine Research, Columbusstraße, 27568 Bremerhaven, Germany* and
[2]*Physical Chemistry, School of Pharmacy and Biochemistry, University of Buenos Aires, Buenos Aires, Argentina*

*Author for correspondence (e-mail: abele@awi-bremerhaven.de)

Summary

Mitochondrial respiration, energetic coupling to phosphorylation and the production of reactive oxygen species (ROS) were studied in mitochondria isolated from the eurythermal bivalve *Mya arenaria* (Myoidea) from a low-shore intertidal population of the German Wadden Sea. Measurements were conducted both within the range of the habitat temperatures (5–15 °C) and when subjected to heat exposure at 20 °C and 25 °C. Experimental warming resulted in an increase in the rate of state 3 and state 4 respiration in isolated mitochondria. The highest respiratory coupling ratios (RCR) were found at 15 °C; at higher temperatures mitochondrial coupling decreased, and release of ROS doubled between 15 and 25 °C. ROS production was 2–3 % of total oxygen consumption in state 3 (0.3–0.5 nmol ROS mg^{-1} protein min^{-1}) at the habitat temperature, reaching a maximum of 4.3 % of state 3 respiration and 7 % of oligomycin-induced state 4+ respiration under heat stress. Thus, state 4 respiration, previously interpreted exclusively as a measure of proton leakage, included a significant contribution from ROS formation in this animal, especially under conditions of heat stress. Oxygen radical formation was directly dependent on temperature-controlled respiration rates in states 3 and 4 and inversely related to mitochondrial coupling (RCR+) in state 4. Mitochondrial ROS formation is therefore involved in cellular heat stress in this eurythermal marine ectotherm.

Key words: mitochondrial function, reactive oxygen species, heat stress, antioxidant, mud clam, *Mya arenaria*.

Introduction

In the context of global warming and its anticipated effects on the marine biosphere, the thermal tolerance limits of marine ectotherms and the metabolic features that determine these limits have generated considerable interest. Not only the temperature extremes but also the high thermal fluctuations, characteristic of intertidal mudflats, affect the energy metabolism of ectothermal animals inhabiting these areas. Many eurythermal species adjust their metabolic rates to the prevailing habitat temperatures; however, the scope for metabolic adjustment depends on the functional capacity of ventilation and circulation, which is limited to a particular thermal tolerance window for a species or a population and, thus, sets limits to its geographical distribution (Pörtner, 2001). Constraints occur with respect to tissue oxygenation and to mitochondrial function and energy production, both of which are reduced at critically high temperatures (Pörtner et al., 1999b; Frederich and Pörtner, 2000). In the whole animal, switching on mitochondrial anaerobic energy production indicates oxygen deficiency at temperatures beyond both the low and high critical thresholds (Pörtner, 2001).

Thermal stress is also accompanied by oxidative stress in various marine mollusc species (Abele et al., 1998, 2001). These findings were based on indirect measurements of oxidative stress, such as malonedialdehyde and lipofuscin accumulation in the tissues (Abele et al., 1998), or changes in antioxidant enzyme activities upon heating (Abele et al., 1998, 2001). Reactive oxygen species (ROS) are normal byproducts of cellular respiration (Boveris et al., 1972), but little is known about oxygen radical formation in invertebrates and virtually nothing about marine invertebrate mitochondria. Mitochondria, respiring in state 3 and in state 4, generate ROS at respiratory chain complexes I (exogenous NADH dehydrogenase; Turrens and Boveris, 1980) and III (ubiquinone, UQ/cytochrome *b* complex; Boveris and Chance, 1973; Cadenas et al., 1977; Han et al., 2001). Elevated rates of ROS production by ubisemiquinone radicals (UQ$^{\bullet-}$) are promoted in resting state 4 of isolated mitochondria, following complete phosphorylation of ADP (Loschen et al., 1971; Boveris and Chance, 1973) (for a review see Skulachev, 1996). Under these conditions, intracellular oxygen concentrations increase, because cytochrome *c* oxidase activity is low, while the proton potential across the inner mitochondrial membrane ($\Delta\mu H^+$) is maximal. Mitochondrial ROS production is described to be a direct function of $\Delta\mu H^+$ (Skulachev, 1998) and to be controlled by 'mild uncoupling' *via* proton leakage through the inner mitochondrial membrane. Moreover,

increased production of reactive oxygen species was detected after the addition of the respiratory chain blocker antimycin a (Boveris and Chance, 1973; Loschen et al., 1973; Boveris and Cadenas, 1975) and, generally, when respiratory chain components are in a maximally reduced state, e.g. under hypoxic conditions.

According to Brookes et al. (1998), the mitochondria of ectotherms generally exhibit a lower membrane potential, lower proton leakage and lower rates of substrate oxidation and, therefore, an overall reduced rate of state 4 respiration compared to endotherms. This goes hand in hand with reduced rates of state 3 respiration. Indeed, the rate of mitochondrial oxygen consumption of invertebrates and ectothermic vertebrates in all functional states is low compared with that of mammals and birds on a mitochondrial protein basis. This may not, however, necessarily be true with respect to ROS production in vertebrate and invertebrate mitochondria.

ROS are not only byproducts of mitochondrial respiration, but can also be detrimental to the generating cell itself if not extinguished or expelled, so it is interesting to study mitochondrial localization in ROS-generating cell types. Superoxide anion radicals ($O_2^{\bullet-}$) are converted to membrane-permeable H_2O_2 by mitochondrial superoxide dismutase, enabling diffusion of peroxide to the extracellular space and the body fluids and, eventually, release to the outer environment through gill diffusion. Clustering of mitochondria at the cellular border would keep diffusion distances short and limit H_2O_2-related damage in the centre of the cell.

The present study was designed to examine mitochondrial ROS production in a marine invertebrate species, the intertidal mud clam *Mya arenaria*. ROS production was measured in intact and well-coupled isolated mitochondria in respiratory states 3 and 4 and related to mitochondrial respiration, the respiratory coupling ratio (RCR) and the efficiency of phosphorylation (ADP:O ratio) with malate as respiratory substrate. Measurements were conducted over the temperature range 5–25 °C, covering the habitat temperature range (5–18 °C) as well as higher temperatures that pose a heat stress to these animals. Correlated changes in antioxidative defence were investigated by testing the effects of temperature on the antioxidant enzymes catalase and superoxide dismutase *in vitro*, and in an experiment with intact animals exposed to habitat and higher temperatures. Specifically, the following questions were addressed. (i) Does temperature stress imply significant increase of ROS production in mitochondria of marine ectotherms? (ii) Is ROS formation primarily related to the functional state of the mitochondria (state 3 *versus* state 4 respiration) and does it depend on the level of proton leak, i.e. mild uncoupling of the proton potential ($\Delta\mu H^+$) in a eurythermal ectotherm under heat stress? (iii) Given that the rate of ROS formation increases at high temperatures, does the organism strive to control it either by increasing the leak or by increasing the antioxidant defence? (iv) Are mitochondria evenly distributed or clustered in these cells and does the distribution indicate which cellular structures might be affected by release of active oxygen species?

Materials and methods

Animal collection and maintenance

Bivalves of the species *Mya arenaria* L. (3–6 cm shell length) were dug on an intertidal sandflat near Bremerhaven, Germany, at the beginning of March 2000. In the laboratory, animals were kept at 10 °C in natural aerated sea water of 23–26 ‰ salinity in aquaria without sediment for 1 week prior to experiments and throughout the experimental time of 3 weeks. The animals were fed phytoplankton once a week.

Isolation of mitochondria

Mitochondria were isolated from mantle tissue of freshly killed *Mya arenaria*. Approximately 4 g of mantle tissue from 6–8 individuals were washed and finely chopped in 10 ml of ice-cold homogenization buffer (400 mmol l^{-1} sucrose, 100 mmol l^{-1} KCl, 6 mmol l^{-1} EGTA, 3 mmol l^{-1} EDTA, 70 mmol l^{-1} Hepes, 1 µg ml^{-1} aprotinin, 1 % bovine serum albumin, BSA, at pH 7.6) modified after Moyes et al. (1985). Extraction of mitochondria was achieved by three passes (200 revs min^{-1}) in a pre-cooled glass/Teflon homogenizer in a total volume of 45 ml homogenization buffer. The homogenate was centrifuged at 1300 g and 4 °C for 14 min, and the supernatant collected and centrifuged again at 10 000 g for 16 min to sediment the mitochondria. The resulting pellet was resuspended in 4 ml of assay medium (560 mmol l^{-1} sucrose, 100 mmol l^{-1} KCl, 10 mmol l^{-1} KH$_2$PO$_4$, 70 mmol l^{-1} Hepes, 5 mmol l^{-1} glutamate, 1 µg aprotinin and 1 % BSA at pH 7.6). This suspension of isolated mitochondria could be kept on ice with no apparent loss of respiratory activity for up to 7 h.

Measurements of mitochondrial respiration and coupling

The measurements of mitochondrial respiration were carried out in thermostatted respiration chambers with an adjustable sample volume of 1–2 ml using Clarke oxygen electrodes and an Eschweiler M200 oxymeter connected to a Linseis two-channel chart recorder. For each measurement, the chambers were filled with 680–880 µl of O$_2$-saturated assay medium, omitting BSA and aprotinin, to which 100–300 µl of mitochondrial suspension and 5 µmol l^{-1} of the myokinase inhibitor P^1,P^5-diadenosine-5′-pentaphosphate (AP$_5$A) in water were added. Rates of oxygen consumption were measured at constant temperature while continuously stirring the mitochondrial suspension at 350 revs min^{-1}. State 2 respiration was initiated by adding 3.3 mmol l^{-1} of the respiratory substrate malate. After approximately 5 min, ADP was added at a final concentration of 0.06 mmol l^{-1} to start state 3 respiration under saturating conditions. State 4 respiration was recorded after the ADP had been consumed (Chance and Williams, 1955). After addition of 2 µg ml^{-1} of the ATPase inhibitor oligomycin, state 4+ respiration was recorded which, according to Brand et al. (1994), reflects the rate of proton leakage. Measurements were carried out at 5, 10, 15, 20 and 25 °C.

The oxygen solubility (β_{O_2}) of the assay medium at experimental temperatures was taken from Johnston et al. (1994). Oxygen consumption ($\dot{M}_{O_2}$) measurements were

corrected for electrode drift at 100 % P_{O_2} and at 0 % P_{O_2}. The respiratory control ratio (RCR) was calculated by dividing state 3 by state 4 respiration according to Estabrook (1967) or by state 4+ respiration following Pörtner et al. (1999a). ADP/O ratios were calculated by dividing the amount of ADP added by the amount of molecular oxygen consumed during state 3 respiration (Chance and Williams, 1955).

Fluorimetric measurements of mitochondrial radical formation

The formation of mitochondrial reactive oxygen species (ROS) was measured at the same time as oxygen consumption in the same mitochondrial isolates using the fluorescent dye dihydrorhodamine-123 (DHR). DHR is non-fluorescent and is oxidized to the fluorescent rhodamine-123 by various reactive oxygen species. We tested the fluorophore with and without peroxidase and found that this enzyme is not required as cofactor. The fluorescence signal was detected using a thermostatted spectrofluorometer (Perkin & Elmer LS 50B) at an excitation wavelength of 505 nm and emission wavelength of 534 nm (excitation slit 2.5 nm, emission slit 3.5 nm). DHR ($14.4 \, mmol \, l^{-1}$) was dissolved in dimethylsulphoxide (DMSO), which had previously been purged with nitrogen for 30 min. DHR solution ($1.5 \, \mu l \, ml^{-1}$) was added to the assay medium without BSA or aprotinin and gently stirred with a magnetic stirrer, resulting in a final concentration of approximately $20 \, \mu mol \, l^{-1}$. Subsequently, the assay medium containing the DHR was kept in the dark and at the different measuring temperatures.

The assay was performed with 640–840 μl of DHR-containing medium in a thermostatted cuvette with constant slow stirring. Recording was started after adding 150–300 μl of the mitochondrial suspension. Radical formation was measured during state 3 respiration after adding $0.06 \, mmol \, l^{-1}$ ADP. After a 10 min delay, $2 \, \mu g \, ml^{-1}$ oligomycin was added to stop ATPase activity and to initiate state 4+ respiration. This procedure determined the start of state 4 respiration, which could not be detected with sufficient precision in the DHR assay. Each state was recorded for at least 10 min.

Calibration of the dihydrorhodamine-123 assay for ROS formation in mitochondrial isolates

DHR oxidation by ROS was quantified using $50 \, \mu mol \, l^{-1}$ xanthine/xanthine oxidase (XOD) to yield a constant rate of formation of oxygen radicals, which reduce the oxidized form of cytochrome c ($100 \, \mu mol \, l^{-1}$). Calibration was performed in the assay medium at temperatures between 5 and 25 °C in a thermostatted spectrophotometer. At each temperature, xanthine oxidase was added at concentrations of 0.75–16 mU and the reduction of cytochrome c was measured.

At 25 °C in a $50 \, mmol \, l^{-1}$ phosphate buffer at pH 8.5, one unit of XOD converts 1 μmol of xanthine to uric acid, producing approximately the same amount of superoxide anions for the reduction of cytochrome c. Since our measurements were performed in the mitochondrial assay medium at pH 7.6, the rate of oxygen radical production was calculated directly from the measured rate of reduction of cytochrome c using the millimolar extinction coefficient ε (550 nm) of 28.5. A linear correlation ($r^2=0.995$; $N=5$) was found between added XOD activity (A_{XOD}) (milliunits ml^{-1}) and the resulting cytochrome c reduction, from which the rate of ROS production (R_{ROS}) ($\mu mol \, l^{-1} \, min^{-1}$) could be calculated:

$$R_{ROS}=0.0677A_{XOD} \text{ at } 10 \, ^\circ C \qquad (1)$$

and

$$R_{ROS}=0.0802A_{XOD} \text{ at } 15 \, ^\circ C. \qquad (2)$$

The slope of the linear regression increased with temperature ($Q_{10}=2$), and at 25 °C, 1 milliunit of XOD produced approximately 0.2 μmol superoxide anions $l^{-1} \, min^{-1}$.

In a second step, the rate of DHR oxidation was determined with the same XOD/xanthine system at 15 °C to obtain the ratio of superoxide anions (x_{ROS}) ($nmol \, ml^{-1} \, min^{-1}$) produced to the rate of DHR oxidation (S_{DHR}) under assay conditions. The data were best fitted by a second-order polynomial function $x_{ROS}=0.0183(S_{DHR})^2+0.0685S_{DHR}$ ($r^2=0.9906$, $P<0.05$, $N=9$). DHR did not react directly with xanthine oxidase, as observed by Hempel et al. (1999), and was oxidized spontaneously at a very slow rate, irrespective of temperature. To correct for possible variation in the rate of DHR oxidation in individual stock solutions, we measured the slope of each DHR-medium daily, using a standard ROS formation system of 10 μl of xanthine oxidase (3 milliunits ml^{-1}) and $50 \, \mu mol \, l^{-1}$ xanthine at 15 °C. A mean slope was calculated based on all measurements, and the individual DHR slopes recorded on each day were corrected for day-to-day variation (<5 %) from the mean slope.

To identify the reactive oxygen species produced in our mitochondrial assays, we used specific quenchers for $O_2^{\bullet-}$ (SOD), H_2O_2 (catalase) and $OH^\bullet$ ($100 \, mmol \, l^{-1}$ DMSO). Assays were run as described above with intact respiring mitochondria under state 3 conditions (with ADP), as well as with submitochondrial particles (SMPs), derived from mitochondrial suspensions which had been treated for 5 min by ultrasound.

In experiments with intact mitochondria, SOD had no effect on DHR oxidation, whereas catalase abolished 52.5±15 % and DMSO another 10 % of the fluorescence increase (catalase + DMSO: 61.6±13 % total quenching of DHR oxidation; means ± S.D., $N=11$). In experiments with SMPs, application of SOD led to 31±20 % fluorescence quenching ($N=7$), whereas SOD and catalase together abolished 68.3±7 % of DHR fluorescence ($N=7$). Addition of DMSO reduced the fluorescence increment by another 10 % ($N=2$) (means ± S.D.). The rather small effect of DMSO is presumably due to primary quenching of the $OH^\bullet$ precursor H_2O_2.

Thus, in assays with intact mitochondria, hydrogen peroxide is apparently the major component responsible for DHR oxidation. Superoxide anions, which cannot leave intact mitochondria by diffusion, are obviously of minor importance. When SMPs are used in the assays, superoxide anions reduce

DHR to a variable extent, perhaps depending on residual mitochondrial SOD activity in the preparation. Residual oxidation of DHR is assumed to result from other forms of reactive oxygen species such as lipid radicals, not detected with the applied quenchers.

In view of the quenching experiments, the molar rates of DHR oxidation recorded in the experimental work and calculated according to the calibration with the xanthine oxidase/cytochrome c system, were halved to account for the 50 % contribution of H_2O_2 formed during DHR oxidation in the mitochondrial assays. In this way we derived the fraction of the quantitatively most important ROS component produced and exported from the mitochondria, H_2O_2.

Temperature exposure experiment

In May 2000, a laboratory experiment was performed in which one group of animals was exposed by stepwise warming to 18 °C and then to 25 °C, while a control group was kept at constant, low temperatures of 10–12 °C. Animals for this experiment were collected at the end of April 2000 at a habitat temperature of around 10 °C. In the laboratory, animals were kept in aquaria with natural, well-aerated sea water at a salinity of 24–26 ‰ and fed phytoplankton once a week. After 2 weeks at 10 °C, one aquarium with 20 experimental animals was warmed by 1 °C every 2 days, until a final temperature of 18 °C was reached. This plateau was kept for 3 days, after which a first batch of eight animals was killed and samples of mantle tissue, digestive gland and gills were taken. On the same day, eight control animals, maintained at 10 °C, were killed and processed in the same way. The remaining specimens were further warmed from 18 °C to 25 °C, following the same protocol, and kept at this temperature for 7 days (long-term heat stress). A third group was transferred directly from 10 °C to 25 °C and maintained at this temperature for 2 days (short-term heat stress). Each sample of heat-exposed animals was compared with the sample of eight control animals maintained for the same time period at 10 °C. Tissue samples were frozen in liquid nitrogen and kept at –80 °C for up to 2 months prior to analysis.

Measurements of antioxidant enzyme activities and malondialdehyde tissue concentrations

Catalase (CAT; E.C. 1.11.1.6) was extracted into 50 mmol l^{-1} potassium phosphate buffer (pH 7.0, 1:19 w/v) and measured according to Aebi (1985). Superoxide dismutase (SOD; E.C. 1.15.1.1) activity in crude homogenates was measured using the xanthine oxidase/cytochrome c assay according to Livingstone et al. (1992). Enzyme assays were generally carried out at 20 °C and at the temperature at which the animals had been kept. Malondialdehyde (MDA) tissue concentrations were measured as a marker of lipid peroxidation according to Uchiyama and Mihara (1978), as described in Storch et al. (2001). The method was modified only with respect to the heating time of the samples, which was 1 h at 100 °C. Absolute MDA concentrations were calculated using a 5-point calibration curve, obtained as follows: a malondialdehyde-(bis)-acetate standard was diluted 1:4000 with 1.1 % phosphoric acid and left standing for 2 h at room temperature in the dark, to yield a 1.01 mmol l^{-1} MDA solution, which was diluted to concentrations between 0.5 and 50 µmol l^{-1} and processed in the same way as the tissue samples.

Counts and localization of mitochondria with confocal microscopy

A Leica TCS-NT confocal system with an inverted Leica DM IRBE microscope equipped with an argon–krypton laser was used for confocal imaging of mitochondrial density and clustering in cells isolated from *Mya arenaria* mantle and gill tissue. Small samples of mantle and gills tissue (<50 mg) were excised from freshly killed animals on ice. The tissue was transferred to small vials containing 10 µl of Type IA collagenase solution (Sigma) in 2 ml of Hepes Ringer (300 mmol l^{-1} NaCl, 140 mmol l^{-1} KCl, 5 mmol l^{-1} Na$_2$SO$_4$, 10 mmol l^{-1} CaCl$_2$•2H$_2$O, 5 mmol l^{-1} MgCl$_2$•6H$_2$O, 5 mmol l^{-1} Hepes, pH 7.6), cut coarsely with small scissors, and digested at 12 °C for 2 h. Thereafter, cells were separated from the undigested residues by filtering through 300 µm gauze and precipitated by 25 min of centrifugation at 75 g and 12 °C in an Eppendorf centrifuge (5810 R). The cells were washed once with the same Ringer's solution and subsequently stained with organelle-specific dye (MitoTracker Green FM, Molecular Probes) at a concentration of 0.2 nmol ml^{-1} in Ringer for 15 min at room temperature (20 °C). After staining, the cells were again precipitated by centrifugation, resuspended in 50–100 µl of Ringer's solution and kept on ice for subsequent mitochondrial counts. MitoTracker Green stock solution (100 µmol l^{-1}) was prepared in DMSO and frozen in portions of 10 µl at –30 °C until use.

Approximately 30 µl of cell solution was pipetted into a microscope chamber, which was mounted onto the microscope stage of the Leica IRBE confocal microscope and cooled to 12 °C. Cells were imaged with a 100×/1.40–0.70 oil immersion lens with the following properties: excitation wavelength 488 nm, laser power 145, confocal pinhole 0.8, emission filter 530±30 nm, photomultiplier voltage 920, offset –2. A Leica TCS-NT electronic workstation equipped with Leica scanning software was used for digital imaging.

Cells were scanned at 1.4 or 1.5 µm sections in the z-direction, and mitochondria were counted visually in each section. Cell diameters were calculated by multiplying the number of sections by their thickness, and cell volume was calculated as $3/4\pi r^3$, where r is cell radius. Five animals were used for these experiments, and a total of 49 mantle cells and 46 gill cells were examined.

Statistical analyses

All values are given as means ± S.D. Data were plotted as a function of temperature. Arrhenius break temperatures (ABTs) were calculated from two-phase regressions. Two intersecting lines were selected that best fitted the data according to the method of least sum of squares. Significant differences
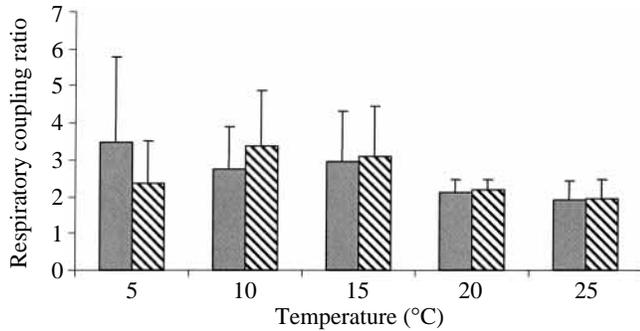
Fig. 1. Comparison of the respiratory coupling ratios (RCR) at different temperatures of isolated mantle mitochondria from *Mya arenaria* determined from the rates of state 3 and state 4 respiration (RCR 3/4; grey columns) and from the rates of state 3 respiration and respiration in the presence of oligomycin (RCR 3/4+; hatched columns); $N=7$–15. RCR 3/4, $P=0.27$ (Kruskal–Wallis ANOVA), RCR3/4+, $P=0.12$ (ANOVA). Values are means ± S.D.

between the resulting slopes were determined by Student's *t*-test. Values of RCR, $\dot{M}_{O_2}$ and ADP/O ratios were tested for homogeneity of variance (Levene test) and normal distribution (Kolmogorov–Smirnov test). If these tests resulted in a statistically significant difference ($P<0.05$), the data were log-transformed. Significant changes in RCR, $\dot{M}_{O_2}$ and ADP/O ratios with temperature were evaluated by analysis of variance (ANOVA) and analysis of covariance (ANCOVA) using Newman–Keuls *post-hoc* comparisons. A non-parametric test (Kruskal–Wallis ANOVA) was used in those cases where transformation did not reveal homogeneity of variance and normal distribution. Differences in enzyme activities and MDA contents of tissue samples from temperature exposure experiments were analysed by Student's *t*-test (using computer programs Super-Anova and Statistica).

Results

Temperature-dependence of mitochondrial functioning

Mya arenaria mitochondria were well coupled over the whole temperature range. The RCR was fairly constant between 3 and 5 at 15 °C (Fig. 1). Upon further warming, the RCR decreased to 1.9±0.5 at 25 °C ($P=0.27$; $N=7$). Mitochondrial state 3 respiration increased significantly over the entire range of investigated temperatures (Fig. 2A, $P=0.023$, $N=8$–18). The maximal rate of state 3 respiration with malate was 15.2±6.3 nmol O min⁻¹ mg⁻¹ mitochondrial protein ($N=8$) at 25 °C. An Arrhenius break temperature (ABT) could be identified as the minimum pooled least sum of squares between 10 and 15 °C. Below 15 °C, the temperature-dependent rise in the rate of state 3 respiration was more pronounced (for 5–10 °C, $Q_{10}=3.22$) than at temperatures above 15 °C (for 15–25 °C, $Q_{10}=1.36$). The same was observed for the amount of oxygen consumed by respiratory activity coupled to phosphorylation, calculated as the rate of state 3 respiration minus the rate of state 4+ (Fig. 2A), which also displayed temperature-dependency only
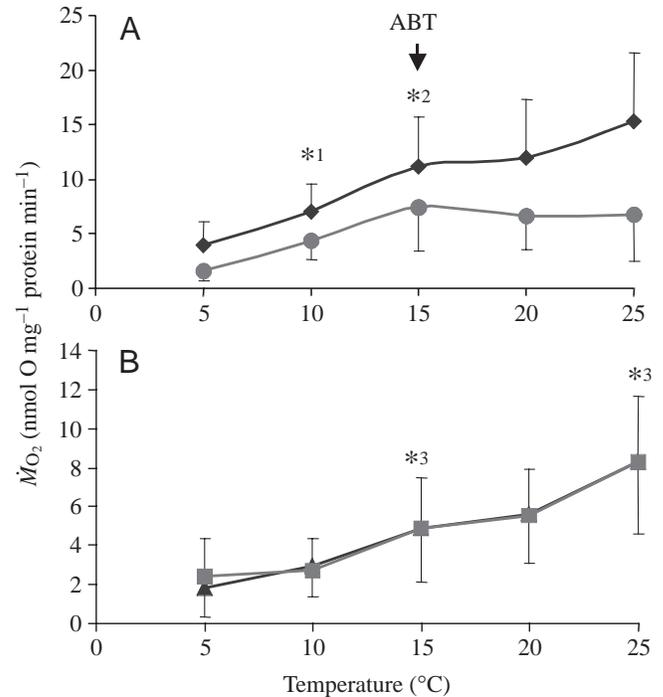
Fig. 2. Temperature-dependence of (A) the rate of state 3 respiration (diamonds) and the difference between the rates of state 3 and state 4+ respiration (circles) and (B) the rate of state 4 respiration (triangles) and state 4+ respiration (squares) of mantle mitochondria from *Mya arenaria*. ABT, Arrhenius break temperature. * indicates values that are significantly different from values at the lower temperature; $N=8$–18. *1 for state 3 and state 3 minus state 4+: $P<0.01$; *2 for state 3: $P=0.023$; *3 for state 4 and state 4+: $P<0.01$. (All ANOVA, ANCOVA; Newman–Keuls test.) Values are means ± S.D.

below 15 °C. Both state 4 respiration ($P<0.01$, $N=8$–18) and oligomycin-insensitive state 4+ respiration ($P<0.01$, $N=8$–18), which is considered to be a measure of proton leakage through the inner mitochondrial membrane, increased significantly between 10 and 15 °C and between 20 and 25 °C (Fig. 2B). Overall state 4 respiration rate was 4.82± 2.6 nmol O mg⁻¹ min⁻¹ ($N=18$) and, thus, approximately 50 % of state 3 respiration rate at 15 °C. There was no difference between state 4 and state 4+ respiration, indicating that ATP generation was complete at the end of state 3 and had stopped in state 4. Together, the continuous increase in the rate of state 4 respiration and the break in the rate of state 3 respiration above 15 °C can explain the observed drop in RCRs above the ABT. ADP:O ratios decreased significantly with temperature ($P<0.01$, Fig. 3) from 2.98±1.13 ($N=11$) at 5 °C to 1.14±0.42 ($N=7$) at 25 °C. This decrease corresponds to the reduced increment of phosphorylation rates derived from state 3 minus state 4+ respiration above 15 °C.

Temperature-dependence of mitochondrial ROS formation (DHR oxidation)

Mitochondrial ROS formation, measured as equivalents of oxidized DHR, increased exponentially (state 3,
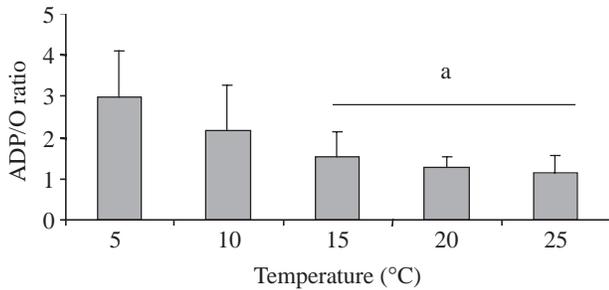
Fig. 3. Dependence of ADP/O ratios of *Mya arenaria* mantle mitochondria on temperature; N=7–16; P<0.01 (ANOVA; Newman–Keuls test). a indicates values significantly different from the value at 5 °C (means ± S.D.).
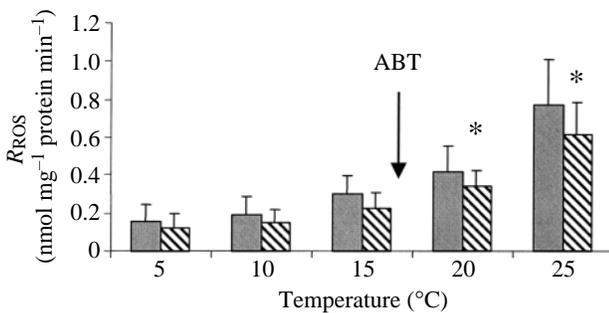
Fig. 4. Temperature dependence of total reactive oxygen species (ROS) formation in *Mya arenaria* mantle mitochondria under state 3 conditions (grey columns) and under state 4+ conditions (hatched columns); N=6–7. Values are means ± S.D. State 3, P<0.01 (Kruskal–Wallis ANOVA); state 4+, P=0.062 (ANCOVA) and P=0.032 (Newman–Keuls test), ABT, Arrhenius break temperature. * indicates values significantly different from values at the 5 °C lower experimental temperature in state 4+.

y=0.096exp(0.392x), r^2=0.972, N=6–7; state 4+, y=0.073exp(0.411x), r^2=0.967, N=6–7) within the investigated temperature range (Fig. 4). The overall increase in mitochondrial ROS formation was significant only in state 3 (Kruskal–Wallis ANOVA, P<0.01), but not-significant in state 4+ (ANCOVA, P=0.062). However, Newman–Keuls *post-hoc* tests yielded a significant increase in state 4+ rate of ROS production between 15 and 20 °C (P=0.032) and between 20 and 25 °C (P<0.01). Overall ROS formation rates were between 0.16±0.09 nmol min^{-1} mg^{-1} (N=6) at 5 °C and 0.76±0.24 nmol min^{-1} mg^{-1} (N=7) at 25 °C in state 3, and between 0.13±0.07 nmol min^{-1} mg^{-1} (N=6) at 5 °C and 0.62±0.17 nmol min^{-1} mg^{-1} (N=7) at 25 °C in state 4+. Analysis of least sum of squares yielded an ABT between 15 °C and 20 °C for states 3 and 4+. Below this ABT, the temperature-dependent increase in the rate of mitochondrial ROS formation was less pronounced and displayed a Q_{10} value of 1.8 in state 3 and 1.9 in state 4+. Above the ABT, the exponential rise resulted in a Q_{10}=3.1 for both states. Arrhenius activation energy (E_a) between 5 °C and 15 °C was 38.9 kJ mol^{-1} in state 3 and 43.4 kJ mol^{-1} for state 4+ ROS
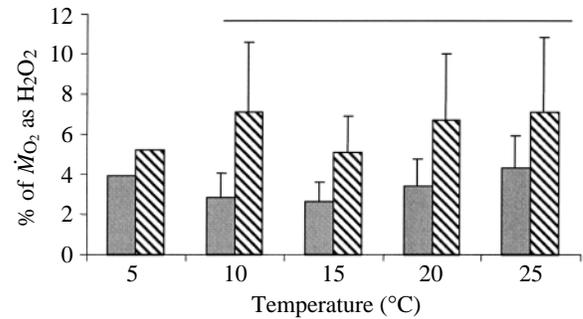
Fig. 5. Temperature-dependence of percentage of total oxygen converted to hydrogen peroxide (% of $\dot{M}_{O_2}$ as H_2O_2) by *Mya arenaria* mantle mitochondria under state 3 conditions (grey columns) and under state 4+ conditions (hatched columns). N=5–7. Values are means ± S.D. state 3, P=0.16 (ANOVA), state 4+, P=0.72 (ANOVA). The line indicates a significant difference between state 3 and state 4+; P<0.01; N=107.

production rate. Above the break temperature, E_a was approximately 80 kJ mol^{-1} in both states.

Rates of mitochondrial respiration and ROS production increased with temperature. Both variables, moreover, correlated significantly with one another in state 3 (Spearman correlation for non-normalized data: r-Spearman=0.74; P<0.01; N=31), and in state 4+ (r-Spearman=0.77; P<0.01; N=31).

The percentage of total oxygen converted to hydrogen peroxide as the major ROS during respiration was calculated on the basis of catalase quenching of DHR oxidation in the mitochondrial assays (Fig. 5). The proportion of hydrogen peroxide formation was significantly higher in state 4+ than in state 3 (P<0.01). The lowest percentage H_2O_2 production from total oxygen consumption was measured at 15 °C and was 2.7±0.98 % (N=5) in state 3 and to 5.12±1.76 % (N=5) in state 4+. Higher percentage values were found both at higher and at lower temperatures. Maximal conversion of oxygen to H_2O_2 was found under state 4 conditions at 25 °C, at which approximately 7 % of the oxygen consumed formed hydrogen peroxide. The dependency of H_2O_2 production on temperature was not, however, statistically significant (P=0.16 for state 3 and P=0.72 for state 4+ respiration, Fig. 5). H_2O_2 production in state 4+ correlated inversely with mitochondrial coupling (RCR+: y=−0.51x+0.6237, r=0.26, P<0.01), indicating that the greater the coupling between respiration and phosphorylation, the lower the production and release of hydrogen peroxide from the mitochondria after inhibition of the ATPase by oligomycin.

Experimental warming of live animals: effects on antioxidant enzyme activities

Adult individuals of *Mya arenaria* with a shell length of 4.5–6 cm were exposed to warming under experimental conditions (Fig. 6). Stepwise warming to 18 °C, which is the maximal temperature recorded naturally in the vicinity of the animals, with a subsequent plateau of 2 days at 18 °C (t-1,
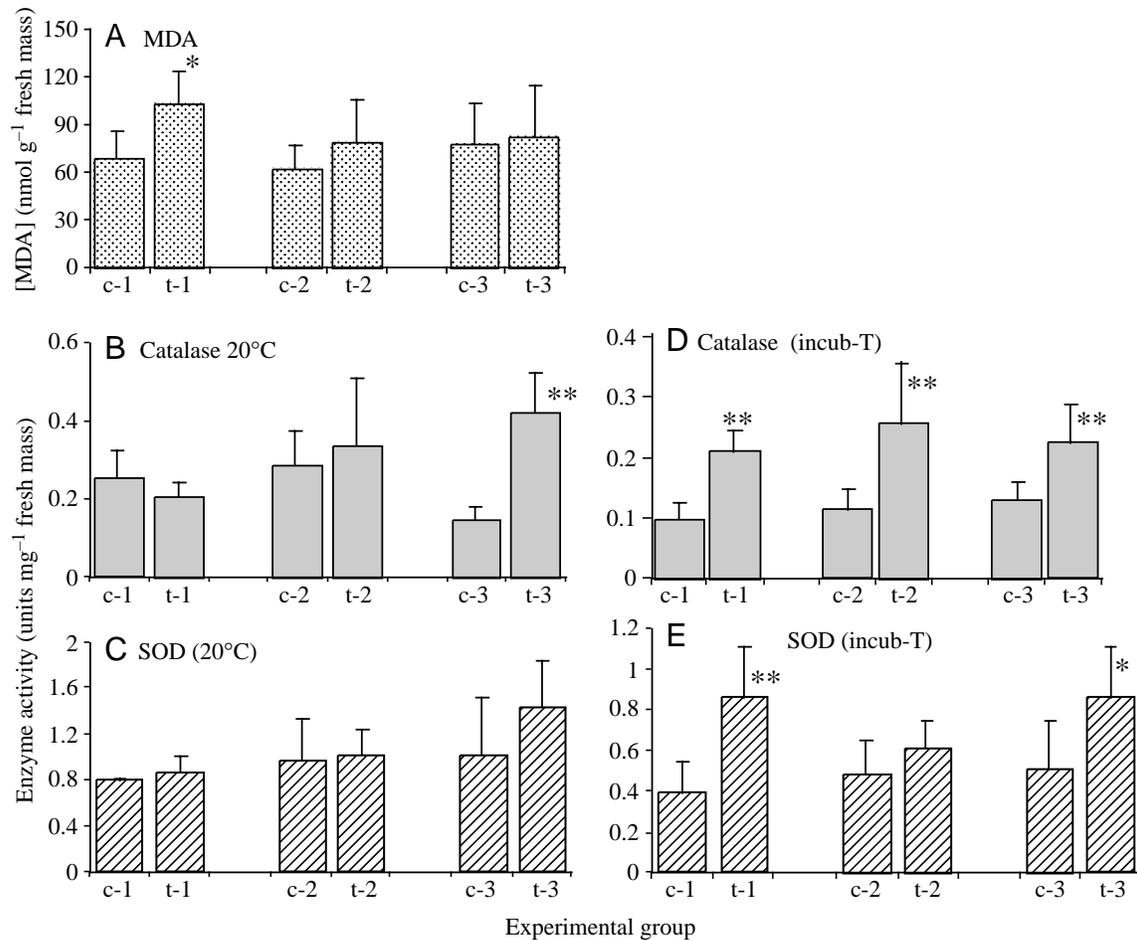
Fig. 6. Malonedialdehyde (MDA) concentrations and AOX (catalase and superoxide dismutase, SOD) activities in *Mya arenaria* tissues after experimental warming of live animals. Experimental groups: t-1, stepwise warming to 18 °C; t-2, stepwise warming to 25 °C (1 °C per day), t-3, direct transfer from 10 to 25 °C (heat stress); c-1 to c-3, respective controls kept at constant 10 °C for the same time as the 'temperature groups'. Measurements were taken at 20 °C (B,C) and at the respective maintenance temperature (incub-T) (D,E). (A) malonedialdehyde concentrations (MDA) in mantle tissue, (B,D) catalase mantle tissue, (C,E) SOD gill tissue. Data are means ± S.D. from 4–10 animals, *$P<0.05$, **$P<0.01$, values significantly different from controls.

Fig. 6A), led to a significant increase in MDA concentrations in mantle tissue compared with controls (c-1) ($P=0.03$; $N=4$ controls, $N=7$ experimental animals), whereas no effect was found with respect to catalase or SOD activities in mantle and gill tissues when all samples were assayed at 20 °C (Fig. 6B,C). When the control group samples were assayed at 10 °C and compared with the 18 °C temperature group (assayed at 20 °C), SOD and catalase activities were significantly higher in the warmed than in the control group (SOD, $P=0.02$, $N=4$ controls, $N=6$ experimental animals; catalase, $P<0.001$, $N=6$ controls, $N=7$ experimental animals, Fig. 6D,E).

Stepwise slow acclimation to 18 °C followed by a 1 week plateau at 25 °C in a second group had no significant effect on antioxidant enzyme activities when assayed at 20 °C (Fig. 6B,C: c-2 and t-2). When assayed at the respective maintenance temperatures (incub-T), only catalase displayed significantly higher enzyme activities as a result of slow warming (Fig. 6D, $P<0.01$, $N=8$ controls, $N=9$ experimental animals), while SOD was unaffected (Fig. 6E, $P=0.15$, $N=7$

controls, $N=9$ experimental animals). MDA concentrations in the mantle tissue increased upon slow warming, but the difference between heated and control animals was not significant (Fig. 6A, $P=0.72$, $N=7$ controls, $N=8$ experimental animals). The third group was transferred directly from 10 to 25 °C and kept at that temperature for 2 days, representing short-term exposure to above habitat temperatures. This treatment resulted in a highly significant increase in catalase activity in the mantle tissue (Fig. 6B,c-3 and t-3, $P<0.01$, $N=6$ controls, $N=9$ experimental animals) and to a non-significant increase in SOD activity in gill tissues (Fig. 6C, $P=0.099$, $N=8$ controls, $N=10$ experimental animals), when assayed at 20 °C. When the enzymes were assayed at the respective exposure temperatures, both antioxidant enzyme activities increased significantly with respect to controls (catalase, $P=0.003$; SOD, $P=0.014$, $N=6$–9, Fig. 6D,E). MDA tissue concentrations did not differ between the control and heated groups (Fig. 6A, $N=8$ controls, $N=9$ experimental animals).
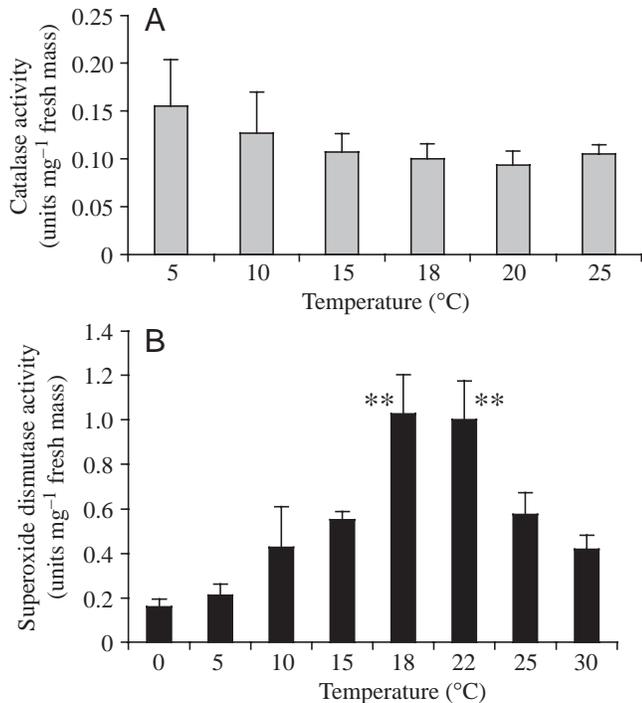
Fig. 7. Temperature profiles of antioxidant enzyme activities in *Mya arenaria* in vitro (units mg fresh mass). (A) Catalase in mantle tissues, (B) superoxide dismutase in gill tissues. Values are means ± S.D., N=5–8. **Values at 18 and 22 °C in B are significantly different from those at all other temperatures ($P<0.01$).

Fig. 8. Confocal image of mitochondrial clustering in *Mya arenaria* mantle cells. Staining with MitoTracker green FM (Molecular Probes). Mitochondria (stained yellow) are located periferal and around the nucleus. Scale bar, 10 μm.

Enzyme activity versus *temperature* in vitro

In vitro measurements of the temperature-dependency of catalase and SOD activities were performed in the tissue extracts used in the temperature-exposure experiment (Fig. 7). The temperature/activity curve for catalase in *M. arenaria* mantle tissue is depicted in Fig. 7A. No clearcut temperature-dependency of *in vitro* catalase activity was found. Although tissues of early summer animals, collected in June 2001 from the Wadden Sea were used, highest activities were found at 5 and 10 °C. However, the variability among samples was so high that no significant temperature maximum could be identified. In contrast, SOD activity in gill tissues was significantly dependent on temperature, with maximum *in vitro* activity at 18 and 22 °C compared with all other temperatures (Fig. 7B).

Cell size and mitochondrial density and clustering

The mean cell volume of mantle cells was 300 μm^3, whereas gill cells had a volume of only approximately 200 μm^3. Mean mitochondrial density was 39±18 per mantle cell (N=49 cells) and 34±15 per gill cell (N=46 cells). Mitochondria were clustered in the periphery of the cell close to the cellular membrane and around the nucleus (Fig. 8).

Discussion
Mechanisms of mitochondrial ROS formation

State 4+ respiration in the presence of oligomycin has been regarded to date as a fairly good measure of proton leak (Brand et al., 1994; Pörtner et al., 1999a). Furthermore, ROS formation does not lead to ADP phosphorylation and is insensitive to oligomycin and, therefore, forms another, although quantitatively smaller, part of state 4+ respiration. The proportion of ROS formation in *Mya arenaria* may reach up to 5 % and 7 % under state 4 conditions, hence the contribution of ROS formation to non-phosphorylating respiration should always be considered, especially under conditions when ROS formation might be stimulated.

Like the proton leak, ROS formation in the mitochondrial respiratory chain will contribute to overall rate of mitochondrial oxygen consumption in state 3, depending on proton-motive force, and especially under state 4 conditions, when $\Delta\mu H^+$ is high. In contrast to the leak, mitochondrial ROS production is, to some extent, stimulated by the rate of energy turnover of the cell, as it depends on electron flux through the critical respiratory complexes I and III in all functional states. During the transition from state 3 to state 4 respiration, electron flux and also ROS formation decrease. These decreases lead, however, to a higher proton-motive force and, in consequence, a higher reduction state of the ubisemiquinol (CoQH$^•$) pool, which will favour the transfer of electrons to O$_2$ (Skulachev, 1998). High $\Delta\mu H^+$ inhibits the Q cycle and thereby prolongs the lifetime of the semiquinole (CoQH$^•$). Autoxidation of CoQH$^•$ initiates chain reactions producing superoxide anions, which are converted to H$_2$O$_2$ by SOD and then to the hazardous OH$^•$, thus leading to a relative increase in ROS production under state 4 conditions. This becomes evident when the percentage of ROS formation of total $\dot{M}_{O_2}$ is considered, which increases upon state 3 to state 4 transition. In *M. arenaria* mitochondria, ROS production was

2–4 % in state 3 and increased to 4–5 % in state 4 at habitat temperatures.

Uncouplers have been found to abolish state 4 ROS formation in mammalian heart mitochondria (Korshunov et al., 1997), proving the general dependence of mitochondrial ROS formation on proton-motive force. According to Skulachev (1998), $\Delta\mu H^+$ has a stronger influence than the electron transport rate on ROS formation rates in the respiratory chain. Nonetheless, the rate of state 3 respiration in *M. arenaria* mitochondria correlated significantly with the rate of ROS formation, indicating a major dependency of ROS formation on overall mitochondrial oxygen consumption.

ROS formation and proton leak in mitochondria from endotherms and ectotherms

Initial studies of ROS production by vertebrate heart mitochondria *in vitro* report relatively high rates of 2–3.5 nmol H_2O_2 min^{-1} mg^{-1} mitochondrial protein under non-phosphorylating (state 4) conditions (Boveris and Cadenas, 1975). Other studies report lower values of 0.01–0.15 nmol H_2O_2 min^{-1} mg^{-1} mitochondrial protein in liver mitochondria of various mammalian species during state 4 respiration (Sohal et al., 1990), whereas state 3 production rates of 0.3–0.6 nmol H_2O_2 min^{-1} mg^{-1} mitochondrial protein were measured in rat liver mitochondria (Boveris and Chance, 1973) and 0.5 nmol H_2O_2 min^{-1} mg^{-1} mitochondrial protein in rat heart mitochondria (Hansford et al., 1997). A single study of H_2O_2 production rates in invertebrate mitochondria reports values of 0.8–2 nmol min^{-1} mg^{-1} mitochondrial protein under state 4 *in vitro* conditions in the house fly, *Musca domestica* (Sohal, 1991).

The rate of ROS production in *M. arenaria* at a habitat temperature of 15 °C (state 3, 0.3 nmol H_2O_2 min^{-1} mg^{-1} protein; state 4+, 0.23 nmol H_2O_2 min^{-1} mg^{-1} protein) was within the range reported for mammalian mitochondria at assay temperatures above 20 °C and up to 37 °C (Boveris et al., 1972; Nohl and Hegner, 1978; Hansford et al., 1997). However, even when only the fraction of catalase-sensitive DHR oxidation is considered, the proportion of total oxygen uptake converted to H_2O_2 in *Mya arenaria* mitochondria under state 4 conditions appears to be substantially higher than in mammalian mitochondria. As total respiration in the bivalve mitochondria amounts to only about 10 % of mammalian mitochondrial respiration (e.g. from bovine heart; see Tschischka et al., 2000), the percentage conversion of oxygen to ROS must be comparatively higher. Thus, a percentage fraction of hydrogen peroxide production of 2–3 %, generally valid for mammalian mitochondria at 25 °C, was found only within the habitat temperature range under state 3 conditions (Fig. 5). Under heat stress conditions, ROS production, calculated from the oxidation of DHR, amounted to 5 % of the mitochondrial oxygen turnover under state 3 and up to 7 % under state 4 conditions. Thus, the proportion of conversion of oxygen to ROS is indeed enhanced in the mitochondria of this marine ectothermal species under temperature stress.

Another 10 % of ROS formation quenchable by DMSO and presumably representing OH$^{\bullet}$ radicals, was omitted in this approximation to render our data comparable with the literature reports on H_2O_2 formation. Moreover, the identification of ROS using chemical quenchers is a very crude measure, and more sophisticated analyses are necessary to obtain a clearer picture. Possibly, OH$^{\bullet}$ radicals originate from transition-metal-catalysed decomposition of H_2O_2 in Fenton-like reactions; however, our current knowledge does not permit us to draw a sufficiently detailed picture of the dynamics of ROS formation in *M. arenaria* mitochondria.

According to Brand et al. (1994), the proportion of oxygen consumption used to drive the proton leak (state 4 respiration) is 33±6.8 % of overall mitochondrial respiration in resting rat hepatocytes. In isolated *Mya arenaria* mitochondria, state 4 respiration is 36.8±2.5 % of overall mitochondrial respiration, which represents 30 % of whole-cell respiration at habitat temperatures of 5–15 °C (calculated on a theoretical basis of 20 % surplus cellular non-mitochondrial oxygen consumption; see Brand et al., 1994). These estimates are valid for similar levels of proton-motive force between state 3 and state 4 respiration. They clearly show that, although the nominal values of state 4 oxygen consumption were five- to 20-fold lower in ectotherms, the percentage contribution to $\dot{M}_{O_2}$, despite the high interspecific variability (<10 % in *Sipunculus nudus*; Buchner et al., 2001; up to 50 % of state 3 respiration in *Laternula elliptica*, Pörtner et al., 1999a), is comparable to what is found in endotherms (Brookes et al., 1998).

Mitochondrial functioning and ROS production in Mya arenaria *under heat stress*

As a eurythermal temperate species, *Mya arenaria* exhibits a rather broad window of thermal tolerance (Anderson, 1978). Anderson found a strong temperature-dependence of whole-animal metabolic rate between 5 and 15 °C, while at higher temperatures respiration rates were constant or even decreased. A Q_{10} higher than 3 for mitochondrial state 3 respiration between 10 and 15 ° C below the ABT and the maintenance of RCR and ADP/O ratio within this temperature range, document metabolic maintenance and flexibility within the thermal tolerance window.

Reduced mitochondrial coupling and phosphorylation rates (ADP/O), together with a constant rate of state 3 oxygen consumption and a progressive increase in the rate of non-phosphorylating state 4 respiration above the ABT, are indicative of increased proton leakage across the inner mitochondrial membrane because fewer protons are shunted back *via* the ATPase. Provided that the proton-motive force is similar for state 3 and state 4, the percentage of state 4+ respiration, i.e. proton conductance and ROS formation, of overall state 3 oxygen consumption increases with temperature from 30.8 % (10 °C) to 38 % (15 °C) and 47 % (25 °C). The significant increase in mitochondrial release of partially reduced oxygen (ROS) indicates increased exposure of the cell to hazardous respiratory byproducts under high temperature stress. Thus, mitochondrial ATP production is stagnant above the ABT, whereas futile proton cycling and ROS formation

increase, causing progressive energetic inefficiency and, possibly, oxidative stress at high temperatures (Fig. 3).

Quantitatively, ROS production accounts for only 0.4–0.8 nmol oxygen mg^{-1} protein min^{-1} at 20 and 25 °C and, thus, for no more than 10 % of the non-phosphorylating respiration (state 4). Still, these toxic oxygen compounds (mainly H_2O_2) are obviously not detoxified inside the mitochondria, but are released into the cytosol and may have harmful effects on mitochondrial membranes and other cellular components. Mitochondrial distribution in the mantle cells was clearly peripheral, indicating that the cellular membranes and any type of integral protein might also be damaged.

The whole animal responded to temperature-induced ROS formation by increasing the activity of antioxidant enzymes (AOX) only when specimens were exposed to heat stress by rapid warming above habitat temperature. This is a further indication that these cells are unable to suppress ROS formation during heating and that adaptational processes including AOX synthesis are then required to control the damaging effects of the radicals produced. Increased AOX activity was not found under mild experimental warming to 20 °C, however, indicating that the antioxidant potential still suffices to prevent ROS damage at high, but close to habitat, temperatures. Indeed, the SOD proteins in the gills (and also catalase in this tissue; data not shown) exhibit maximum catalytic activity between 18 and 22 °C. Thus, the animals obviously have no need to invest into AOX synthesis upon mild warming.

Slow warming and acclimation to 25 °C over 7 days also failed to induce elevated tissue AOX levels at the end of the treatment. From the existing data, it is not clear whether a transient induction of AOX has occurred, or if there is any tissue damage. MDA levels in the tissues were only insignificantly increased after the long-term heat exposure, but this might be because MDA is a transient marker of lipid peroxidation, which is incorporated into ageing pigments and also possibly released into the incubation water (McAnulty and Waller, 1999). Mortality was not significantly higher in these than in the other temperature-exposed groups, but no further damage markers (lipofuscin, ROS-induced DNA damage or energetic parameters) were assayed to obtain a more comprehensive picture of the physiological state of the animals. The respiration experiments of Anderson (1978) indicate the beginning of respiratory impairment in cold-acclimated low and mid-intertidal specimens during warming to 25 °C. All mechanisms associated with hypoxia or anoxia adaptation may then come into play, including energy-saving strategies resulting in a decrease in protein synthesis. Such a strategy might explain why AOX enzymes were not found to increase during long-term heat exposure in this species.

Perspectives: the role of intracellular P_{O_2}

These considerations suggest that P_{O_2} in the body and cellular fluids plays an important role in the oxidative stress experienced by an organism at extreme temperatures. For practical reasons, however, this investigation, like many others, studied mitochondrial respiration and ROS formation at P_{O_2} values that are high compared with the much lower intracellular *in vivo* P_{O_2} (see Pörtner and Grieshaber, 1993).

In the intact animal, intracellular oxygen concentration, in itself, represents a major hazard to aerobic cells and has to be kept under tight control to prevent the formation of reactive oxygen species. The futile cycling of protons causes mitochondria to be a permanent oxygen sink and, thereby, contributes to low intracellular oxygen tensions. The proton leak also limits an increase in $\Delta\mu H^+$ and, thereby, mitochondrial ROS formation (Skulachev, 1996).

Compared with animals living in environments with constant oxygen levels, tight control of cellular oxygen tension is even more difficult in intertidal animals, such as *Mya arenaria*, that are exposed to large fluctuations of ambient oxygen levels. Usually, animals respond to fluctuating oxygen supply by ventilatory and circulatory control. In oxyconformers, P_{O_2}-dependent respiration of mitochondria also plays a role (Tschischka et al., 2000; Buchner et al., 2001). In the bivalves studied, ventilatory control is maintained by the inhalation of oxygenated sea water through the siphon. Oxygen uptake occurs by diffusion over the small gills and the large surface area of the mantle that lines the valves (Brusca and Brusca, 1990). Diffusive transport through the tissue itself precludes inhomogeneity of the oxygen supply to the cells in the different tissue layers (Jones, 1986). The relative simplicity of this system is obvious and is further supported by the absence of any oxygen-binding protein from the haemolymph and tissues. Moreover, infaunal bivalves such as *Mya arenaria*, especially, live in low-oxygen environments and are ecologically adapted to endure very low environmental P_{O_2} and to survive extended periods of days and weeks of severe hypoxia (Theede, 1973). All of these considerations suggest that mitochondria of *Mya arenaria* may experience a wide range in intracellular oxygen levels and, thus, indicate that further measurements of ROS formation and oxidative stress should be carried out at these values of intracellular P_{O_2} in isolated mitochondria as well as in intact cells. This will allow further evaluation of the dependence of ROS formation on mitochondrial respiration in marine invertebrates *in vivo*.

References

Abele, D., Burlando, B., Viarengo, A. and Pörtner, H. O. (1998). Exposure to elevated temperatures and hydrogen peroxide elicits oxidative stress and antioxidant response in the Antarctic intertidal limpet *Nacella concinna*. *Comp. Biochem. Physiol.* **120B**, 425–435.

Abele, D., Tesch, C., Wencke, P. and Pörtner, H. O. (2001). How do oxidative stress parameters relate to thermal tolerance in the antarctic bivalve *Yoldia eightsi*? *Antarct. Sci.* **13**, 111–118.

Aebi, H. E. (1985). Catalase. In *Methods of Enzymatic Analysis*, vol. VIII (ed. H. U. Bergmeyer), pp. 273–286. Weinheim: Verlag Chemie.

Anderson, G. (1978). Metabolic rate, temperature acclimation and resistance to high temperature of soft-shell clams, *Mya arenaria*, as affected by shore level. *Comp. Biochem. Physiol.* **61A**, 433–438.

Boveris, A., Oshino, N. and Chance, B. (1972). The cellular production of hydrogen peroxide, *Biochem. J.* **128**, 617–630.

Boveris, A. and Chance, B. (1973). The mitochondrial generation of hydrogen peroxide. *Biochem. J.* **134**, 707–716.

Boveris, A. and Cadenas, E. (1975). Mitochondrial production of superoxide anions and its relationship to the antimycin insensitive respiration. *FEBS Lett.* **54**, 311–314.

Brand, M. D., Chien, L.-F., Ainscow, E. K., Rolfe, D. F. S. and Porter, R. K. (1994). The causes and functions of the mitochondrial proton leak. *Biochim. Biophys. Acta* **1187**, 132–139.

Brookes, P. S., Buckingham, J. A., Tenreiro, A. M., Hulbert, A. J. and Brand, M. D. (1998). The proton permeability of the inner membrane of liver mitochondria from ectothermic and endothermic vertebrates and from obese rats: Correlations with standard metabolic rate and phospholipid fatty acid composition. *Comp. Biochem. Physiol.* **119B**, 325–334.

Brusca, R. C. and Brusca, G. J. (1990). *Invertebrates*, chapter 20, *Mollusca*. Sunderland, Mass.: Sinauer Associates, Inc.

Buchner, T., Abele, D. and Pörtner, H. O. (2001). Oxyconformity in the intertidal worm *Sipunculus nudus*: Mitochondrial background and energetic consequences. *Comp. Biochem. Physiol.* **129B**,109–120.

Cadenas, E., Boveris, A., Ragan, C. I. and Stoppani, A. O. M. (1977). Production of superoxide radicals and hydrogen peroxide by NADH-ubiquinone reductase and ubiquinol-cytochrome *c* reductase from beef heart mitochondria. *Arch. Biochem. Biophys.* **180**, 248–257.

Chance, B. and Williams, G. R. (1955). Respiratory enzymes in oxidative phosphorylation. I. Kinetics of oxygen utilization. *J. Biol. Chem.* **217**, 383–393.

Estabrook, R. W. (1967). Mitochondrial respiratory control and the polarographic measurements in mitochondria. *Methods Enzymol.* **10**, 41–47.

Frederich, M. and Pörtner, H. O. (2000). Oxygen limitation of thermal tolerance defined by cardiac and ventilatory performance in the spider crab *Maja squinado*. *Am. J. Physiol.* **279**, R1531–R1538.

Han, D., Williams, E. and Cadenas E. (2001). Mitochondrial respiratory chain-dependent generation of superoxide anion and its release into the intermembrane space. *Biochem. J.* **353**, 411–416.

Hansford, R. G., Hogue, B. A. and Mildaziene, V. (1997). Dependence of H_2O_2 formation by rat heart mitochondria on substrate availability and donor age. *Bioenerg. Biomem.* **29**, 89–95.

Hempel, S. L., Buettner, G. R., O'Malley, Y. Q., Wessels, D. A. and Flaherty, D. M. (1999). Dihydrofluorescein diacetate is superior for detecting intracellular oxidants: comparison with 2′,7′-dichlorodihydrofluorescein diacetate, 5(and 6)-carboxy-2′,7′-Dichlorodihydro-fluorescein diacetate, and dihydrorhodamine-123. *Free Rad. Biol. Med.* **27**, 146–159.

Johnston, I. A., Guderley, H., Franklin, C. E., Crockford, T. and Kamunde, C. (1994). Are mitochondria subject to evolutionary temperature adaptations. *J. Exp. Biol.* **195**, 293–306.

Jones, D. P. (1986). Intracellular diffusion gradients of O_2 and ATP. *Am. J. Physiol.* **250**, C663–C675.

Korshunov, S. S., Skulachev, V. P. and Starkov, A. A. (1997). High protonic potential actuates a mechanism of production of reactive oxygen species in mitochondria. *FEBS Lett.* **416**, 15–18.

Livingstone, D. R., Lips, F., Garcia Martinez, P. and Pipe, R. K. (1992). Antioxidant enzymes in the digestive gland of the common mussel *Mytilus edulis*. *Mar. Biol.* **112**, 265–276.

Loschen, G., Flohé, L. and Chance, B. (1971). Respiratory chain linked H_2O_2 production in pigeon heart mitochondria. *FEBS lett.* **18**, 261–264.

Loschen, G., Azzi, A. and Flohé, L. (1973). Mitochondrial H_2O_2 formation: relationship with energy conservation. *FEBS Lett.* **33**, 84–88.

McAnulty, J. F. and Waller, K. (1999). The effect of quinacrine on oxidative stress in kidney tissue stored at low temperature after warm ischemic injury. *Cryobiology* **39**, 197–204.

Moyes, C. D., Moon, T. W. and Ballantyne, J. S. (1985). Glutamate metabolism in mitochondria from *Mya arenaria* mantle: effects of pH on the role of glutamate dehydrogenase. *J. Exp. Zool.* **236**, 293–301.

Nohl, H. and Hegner, D. (1978). Do mitochondria produce oxygen radicals in vivo? *Eur. J. Biochem.* **82**, 563–567.

Pörtner, H. O. and Grieshaber, M. K. (1993). Critical $P_O(s)$ in oxyconforming and oxyregulating animals: Gas exchange, metabolic rate and the mode of energy production. In *The Vertebrate Gas Transport Cascade: Adaptations to Environment and Mode of Life* (ed. J. E. P. W. Bicudo), pp. 330–357. Boca Raton FL, US: CRC Press Inc.

Pörtner, H. O., Hardewig, I. and Lloyd, S. P. (1999a). Mitochondrial function and critical temperature in the Antarctic bivalva, *Laternula elliptica*. *Comp. Biochem. Physiol.* **124**, 179 –189.

Pörtner, H. O., Peck, L., Zielinski, S. and Conway, L. Z. (1999b). Intracellular pH and energy metabolism in the highly stenothermal Antarctic bivalve *Limopsis marionensis* as a function of ambient temperature. *Polar Biol.* **22**, 17–30.

Pörtner, H. O. (2001). Climate change and temperature-dependent biogeography: oxygen limitation of thermal tolerance in animals. *Naturwissenschaften* **88**, 137–146.

Skulachev, V. P. (1996). Role of uncoupled and non-coupled oxidation in maintenance of safely low levels of oxygen and its one-electron reductants. *Q. Rev. Biophys.* **29**, 169–202.

Skulachev, V. P. (1998). Uncoupling: new approaches to an old problem of bioenergetics. *Biochim. Biophys. Acta* **1363**, 100–124.

Sohal, R. S., Svensson, I. and Brunk, U. T. (1990). Hydrogen peroxide production by liver mitochondria in different species. *Mech. Age Dev.* **53**, 209–215.

Sohal, R. S. (1991). Hydrogen peroxide production by mitochondria may be a biomarker of aging. *Mech. Age Dev.* **60**, 189–198.

Storch, D., Abele, D. and Pörtner, H. O. (2001). The effect of hydrogen peroxide on isolated body wall of the lugworm *Arenicola marina* at different extracellular pH levels. *Comp. Biochem. Physiol. C* **128**, 391–399.

Theede, H. (1973). Comparartive studies on the influence of oxygen deficiency and hydrogen sulphide on marine bottom invertebrates. *Neth. J. Sea Res.* **7**, 244–252.

Tschischka, K., D. Abele and Pörtner, H. O. (2000). Mitochondrial oxyconformity and cold adaptation in the polychaete *Nereis pelagica* and the bivalve *Arctica islandica* from Baltic and White Sea. *J. Exp. Biol.* **203**, 3355–3368.

Turrens, J. F. and Boveris, A. (1980). Generation of superoxide anion by the NADH dehydrogenase of bovine heart mitochondria. *Biochem. J.* **156**, 435–444.

Uchiyama, M. and Mihara, M. (1978). Determination of malonaldehyde precursor in tissues by thiobarbituric acid test. *Anal. Biochem.* **86**, 271–278.